Journal of Applied Electrochemistry (2006) 36:1011–1019
DOI 10.1007/s10800-006-9169-0

Testing of electrochromic materials using symmetrical devices

C. LEFROU[1,*], C. GENTILHOMME[2] and M. AST[2]
[1]*INPG-Ecole Nationale Supérieure d'Electrochimie et d'Electrométallurgie de Grenoble, Laboratoire d'Electrochimie et Physico-chimie des Matériaux et Interfaces, UMR 5631 CNRS-INPG, BP 75 38402, Saint Martin d'Hères, France*
[2]*Saint-Gobain Recherche, 39 Quai Lucien Lefranc, 93 303, Aubervilliers Cedex, France*
*(*author for correspondence, e-mail: christine.lefrou@inpg.fr)*

Received 6 July 2005; accepted in revised form 24 May 2006

Key words: colouration parameters, electrochromic systems, *in situ* studies, iridium oxide, side reactions, tungsten oxide

Abstract

"Symmetric materials" devices, where both electrodes are made of the same electrochromic materials, allow the *in situ* study of side reactions. Each transferred charge that is not used for the expected electrochromic reaction will cause a colour change in the whole symmetric device. Two electrochromic materials, WO_3 and IrO_2, are successively used to show how to obtain information about side reactions such as faradaic efficiency, reversibility and potential limits from the symmetric experiment. This *in situ* approach with a polymer electrolyte shows significant differences compared to results obtained with studies in aqueous electrolytes.

1. Introduction

Almost all the electrochromic large-area windows which have been investigated up to now have a five-layered structure [1–5] which consists of two thin films of different electroactive materials, at least one being electrochromic, separated by an electrolyte and sandwiched between transparent electron-conducting substrates. Because of the very small distance between the two active layers it is very difficult to introduce a reference electrode into the device [6]. Therefore these devices are in most cases two-electrode systems and the control of the cell voltage does not allow monitoring of the potentials of each active layer [7].

Rauh and Cogan [8, 9] have shown how to predict the potential distribution between the two electrodes in different coloured states. These features are strongly related to the manufacturing parameters such as the thicknesses of both active layers and their level of oxidation/reduction when the device is made. The same model, which takes into account the oxidation and reduction potential limits of both materials, allows the determination of the safe cell voltage window and the electrode at which the side reaction occurs. However, this model has always been used with quasi-equilibrium data on active layers in a liquid electrolyte. The behaviour of the layers could be significantly different in a real device working under dynamic conditions.

This work proposes an indirect approach to study, in real conditions, the behaviour of electroactive materials and the effect of side reactions on the limits of oxidation or reduction. When a current is applied to "symmetric materials" devices (cells where the same electrochromic material is used on both electrodes), one electrode darkens while the other electrode bleaches [10]. Thus, the whole device shows almost no electrochromic effect provided no side reaction occurs. In contrast, assuming side reactions are not electrochromic, any change in colouration indicates the presence of side reaction(s). Colorimetric measurements therefore provide indirect information about *in situ* side reactions.

In the following, experimental results on WO_3 and IrO_2 electrochromic materials with protonic conductors devices are shown. Most of the discussion will focus on the IrO_2 results because its known pseudo-capacitive behaviour [6, 8–14] allows an easy link between charge and potential and therefore gives an easier way of understanding results. However, this approach can be applied to all kinds of electrochromic devices, including those where oxides or polymers are used as electroactive or electrolyte layers. If the electrochromic material exhibits a non pseudo-capacitive behaviour, the determination of the insertion isotherm, that is to say the relationship between inserted charge and potential, should then be carried out.

The expected normal reactions for WO_3 and IrO_2 in protonic devices are the following electrochromic insertion of protons, written in the colouring direction:

$$WO_3 + xe^- + xH^+ \rightleftarrows H_xWO_3 \quad (1)$$

$$H_yIrO_2 \rightleftarrows IrO_2 + ye^- + yH^+ \quad (2)$$

For both materials in aqueous liquid electrolytes, the side reactions are water oxidation with oxygen evolution and proton reduction with hydrogen evolution. Different side reactions may occur with an acidic polymer electrolyte. The nature of these side reactions will be discussed. However the goal of this work is not to determine the exact nature of the side reactions but to focus on the consequences of side reactions on the electrochromic properties of the devices.

2. Experimental

The symmetric materials devices used in this work have a five-layered structure where the same electrochromic material, either a WO_3 or IrO_2 thin film, is used on both electrodes.

The transparent electron-conducting layer, deposited on glass, is SnO_2:F with a sheet resistance of 10 $\Omega/\square$ (i.e. for a square device geometry). The WO_3 and IrO_2 layers were deposited by planar DC magnetron sputtering from a metallic (tungsten or iridium) target in an argon/oxygen plasma. The layer thicknesses are indicated in nm: for example a 40/120 IrO_2 device is a symmetrical device with non-symmetric thicknesses (40 nm at the working electrode and 120 nm at the counter electrode side).

All the devices have an area of about 40 cm^2. All the experiments were performed at room temperature. In experiments involving liquid electrolytes, a three-electrode cell was used with a saturated calomel electrode as reference electrode and a 0.25 M H_3PO_4 aqueous solution as electrolyte.

All the symmetric materials devices investigated used a proton-conducting polymer electrolyte made up of a PEO–H_3PO_4 complex. Both layers were precharged (reduced) with a three-electrode potentiostatic configuration in an aqueous acidic electrolyte before assembly. The potential used for this reduction was +0.1 V/SCE for the IrO_2 layers and −0.2/SCE for the WO_3 layers. This preconditioning was required because the as-deposited layers are almost completely oxidized. Therefore if these materials in the completely oxidized state were to be assembled together, the exchanged charged would immediately be with side reactions. The importance of this manufacturing step (often called precharging) is now well documented for most electrochromic devices [15, 16].

This precharging was followed by the usual manufacturing steps (polymer coating, drying and curing in an autoclave). The potential value (in V/SCE) of each electrode in the short-circuited state in the resulting device was then different from the precharging one and was experimentally determined.

In order to obtain a better sensitivity, spectrophotometric measurements were recorded at 550 nm for the IrO_2 devices and 410 nm for the WO_3 ones (the transmittance being respectively named T_{550} and T_{410}).

3. Results and discussion

3.1. *Voltammetry of WO_3 devices*

Figure 1 shows the voltammogram of a 350 nm WO_3 layer in aqueous acidic electrolyte, recorded with a three electrode configuration. It exhibits the expected peak shape in oxidation [1]. In comparison, Figure 2 shows the voltammetric response of a 350/350 WO_3 symmetric device, recorded with a two electrode configuration,

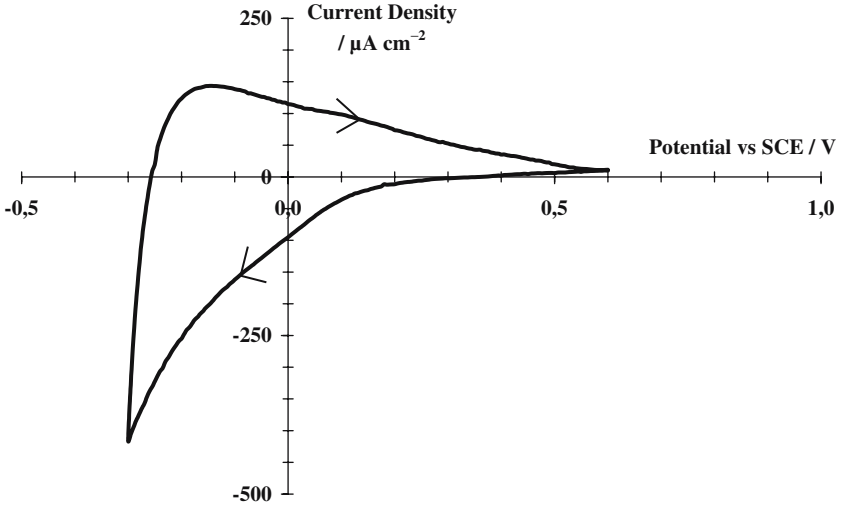

Fig. 1. Cyclic voltammogram for a 350 nm WO_3 recorded at 5 mV s^{-1} in an acidic electrolyte with a three electrode configuration.

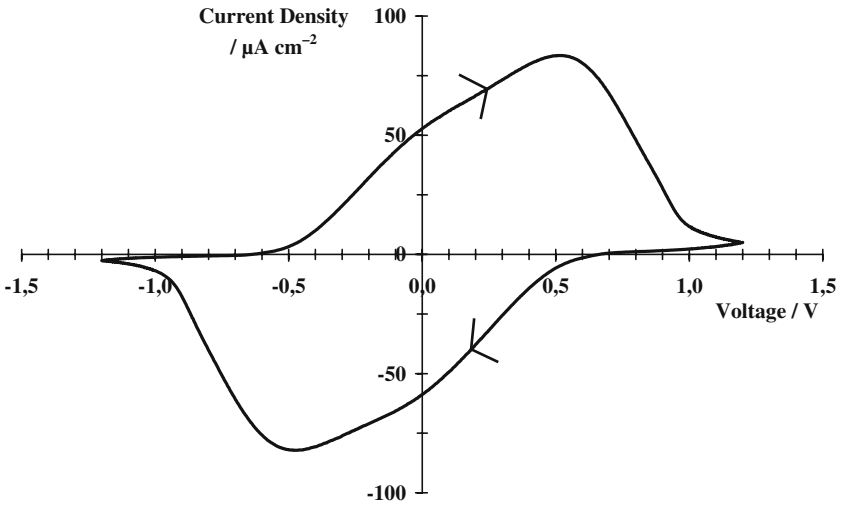

Fig. 2. Cyclic voltammogram for a 350/350 WO_3 symmetric device, recorded at 5 mV s^{-1}.

where only the voltage between the two WO_3 layers is controlled. As expected from the symmetry of the device (same material and same thickness for the two active layers), the voltammogram in Figure 2 is symmetrical about (0,0).

There is no easy quantitative correlation between both experiments. In particular, no specific relationship should be found between the peak positions in both experiments. Experiments on symmetrical devices do not correspond to a regular voltammetric experiment for each individual WO_3 layer. Because of the uncontrolled partition of the voltage between working and counter electrode, the actual scan rate for each layer could be variable and significantly different from that imposed on the whole device.

Nevertheless, a qualitative comparison between both experiments could be done. It is seen from the Figure 1 that the reduction of a WO_3 layer is faster than its oxidation: in the almost completely oxidized state, the potential changes significantly with a very small amount of charge. So, in the symmetric materials device, the oxidation on one side will be the slowest step, reflected in the shape of the voltammogram. For positive voltages, the working electrode monitors the shape whereas for negative voltages the counter-electrode does. With this explanation, the curve shapes and therefore the behaviour of the WO_3 layer in both conditions (oxide/polymer or oxide/liquid electrolyte interface) are qualitatively the same.

In the potential window explored, no side reaction appears to occur: no electrochemical signature of another reaction is observed.

3.2. *Voltammetry of IrO_2 devices*

Figure 3 shows the voltammogram of a 40 nm IrO_2 layer in aqueous acidic electrolyte, with the expected pseudo-capacitive behaviour [13, 14]. In comparison, Figure 4 shows the voltammetric response of a 40/40 and 40/120 IrO_2 symmetric devices. They also exhibit

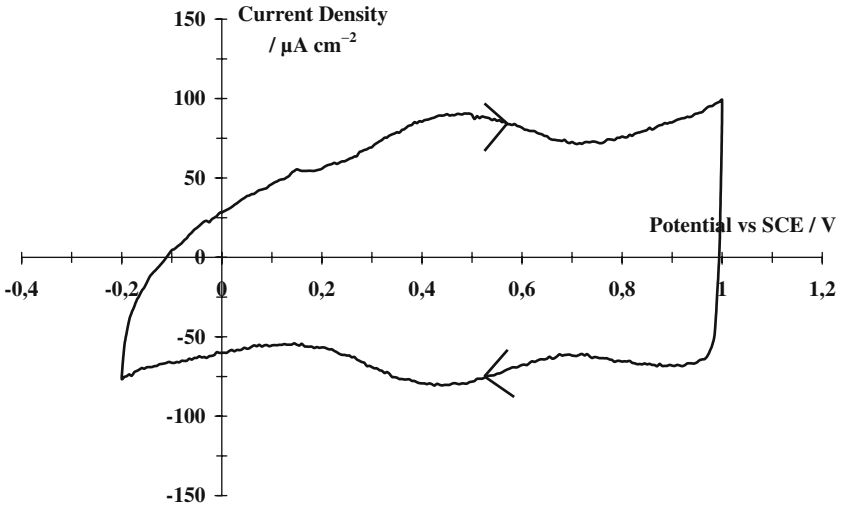

Fig. 3. Cyclic voltammogram for a 40 nm IrO_2 recorded at 5 mV s^{-1} in an acidic electrolyte with a three electrode configuration.

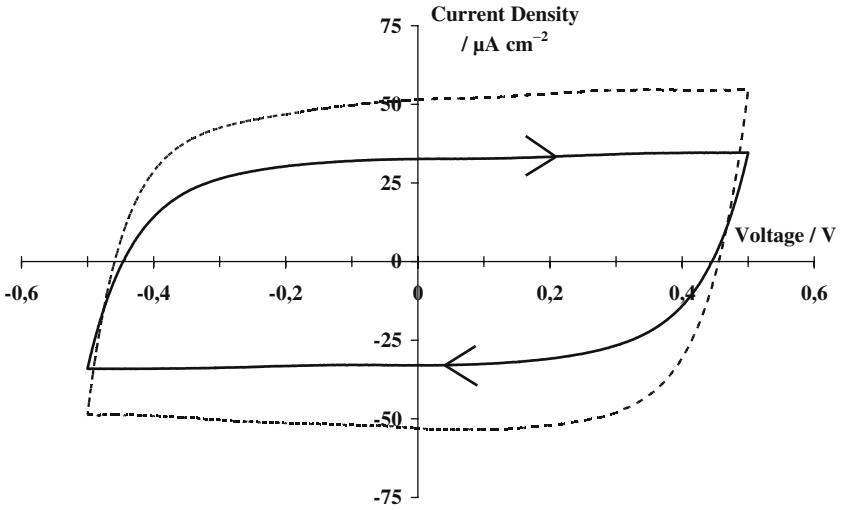

Fig. 4. Cyclic voltammograms for a 40/40 IrO_2 symmetric device (continuous line) and a 40/120 (dotted line) IrO_2 symmetric device, recorded at 5 mV s^{-1}.

pseudo-capacitive behaviour, as expected since a symmetric device is equivalent to a two series pseudo-capacitances circuit: $1/C_{device} = 1/C_{WE} + 1/C_{CE}$.

The pseudo-capacitance C was estimated from the average current I in voltammetric experiments I and the scan rate $v(C = I/v)$, see Table 1. Previous studies show that the pseudo-capacitance of an IrO_2 layer could be considered as proportional to its thickness [6, 8–14]. The equivalent capacitance for a 100 nm IrO_2 layer, C_{100}, is then calculated for each previous experiment (assuming the symmetric device is a two series pseudo-capacitances circuit) and shown in Table 1.

Further experiments could confirm the capacitive behaviour (other voltammetric experiments at various scan rates for example) and the proportionality with the layer thickness, but those points have already been reported [6, 8–14]. Our results show a small decrease in the equivalent pseudo-capacitance when the IrO_2 layer is in contact with the polymer electrolyte (about a 10% decrease). Taunier et al. [6] found opposite results for the same comparison: experiments with a 55 nm IrO_2 layer yielded a C_{100} value of 40 mF cm^{-2} for experiments in acidic liquid electrolyte and 44 mF cm^{-2} in polymer electrolyte. This property seems to depend strongly on the manufacturing steps of the devices (no vacuum drying in this work and no autoclave step in the work of Taunier et al.). However the variations in both studies are small (around 10%) and do not question the discussion proposed in the present work.

3.3. *Occurrence of side reactions*

The voltammetric responses in Figures 2 and 4 do not show the electrochemical signature of a side reaction within the voltage window explored. The transmitance, T_{550}, remained constant (less than 0.2% deviation from the initial value) during the voltammetric sweeps. This quasi-constant colouration suggests that the dynamic conditions used here are slow enough to observe reversible behaviour of the electrochromic reactions with no side-reaction. During charge transfer, one electrode darkens while the other electrode bleaches by exactly the same quantity. Any side-reaction would affect the current efficiency thus creating an imbalance between the colouration of the two layers and modifying the transmittance of the whole device.

3.4. *Colouration efficiency of IrO_2 films*

For almost all electrochromic materials, the colour change can be related to an increase in the number of coloured centers electrochemically produced in the materials. The usual Beer–Lambert law of absorption produces a linear relationship between absorption and charge density, which is proportional to the concentration of coloured centres through Faraday's law. This relationship is usually characterized by the colouration efficiency, defined by the slope of the $Log_{10}(T_{550})$ versus

Table 1. Average current, pseudo-capacitance and equivalent pseudo-capacitance for a 100 nm IrO_2 layer extracted from the different volammetric results on IrO_2

Device	Average current density /μA cm^{-2}	Pseudo-capacitance /mF cm^{-2}	Pseudo-capacitance, C_{100} for a 100 nm layer/mF cm^{-2}
40/40 IrO_2	33	6.6	33
40 IrO_2	≈75	≈15	≈37
40/120 IrO_2	52	10.3	34

Q curve, where Q is the charge density exchanged between two different oxidation states [1–8]. This linear relationship is generally valid up to a few tens of mC cm^{-2}.

The colouration efficiency of the IrO_2 materials was determined with several galvanostatic experiments in liquid electrolyte on both IrO_2 layers (40 and 120 nm thick). Linear variations were observed for both layers up to 20 mC cm^{-2}, with very comparable slopes (13 and 14 $cm^2\ C^{-1}$). In the following discussion, the colouration efficiency will therefore be considered as constant. To allow comparison with results from symmetric devices the colouration efficiency needs to be corrected for the difference in capacitance (see Table 1). The value used will then be: $13.5 \times 37/33.5 = 15\ cm^2\ C^{-1}$. This corrected value is in good agreement with previously published results, which range from 10 to 18 $cm^2\ C^{-1}$ for different IrO_2 thin films [6, 8–12].

3.5. *Symmetric IrO_2 devices under galvanostatic control*

In order to study side reactions, symmetric material devices with non-symmetric thicknesses were used. The thinner layer will almost always be the limiting electrode, where side reactions occur, as discussed further.

Figures 5 and 6 show different galvanostatic experiments on 40/120 IrO_2 symmetric devices. Under these conditions, the charge density is proportional to time. In each case the experiment started from the short-circuited state. Figures 5 and 6 show the transmittance and the voltage variation with time during a galvanostatic experiment at $+20\ \mu A\ cm^{-2}$ and $-20\ \mu A\ cm^{-2}$ respectively. The voltage changes show relatively slow variations: the maximum slope is around 2 mV s^{-1}. The assumption of reversibility of the electrochromic reactions is reasonable in these galvanostatic experiments.

3.6. *Direction of the transmittance variation*

When positive current was applied, the IrO_2 working electrode coloured whereas the IrO_2 counter electrode bleached. The bleaching of the whole device in Figure 5 therefore reveals a side oxidation reaction at the working electrode (40 nm thick): some charge is consumed without colouring the working electrode.

Based on the same argument, the darkening of the whole device in Figure 6 reveals a side reduction reaction at the working electrode: some charge is consumed without bleaching the working electrode.

These experiments indicate that in order to detect side reactions the colouration parameter (T_{550}) is more sensitive than the electrochemical one: i.e. the changes in slope of the voltage variation with time are very slow.

3.7. *Side reaction faradaic efficiency*

Colouration efficiencies, that is to say the slope of the $Log_{10}(T_{550})$ versus Q curve, named η, are available from the transmittance versus time curve after the change of slope (see inset on the Figures 5 and 6, values taken after the second arrow):

$$\text{experiment with positive current} \quad \eta_+ = +7\ cm^2\ C^{-1}$$

$$\text{experiment with negative current} \quad \dot{\eta}_- = -10\ cm^2\ C^{-1}$$

It is then possible to estimate the importance of the side reaction through its faradaic efficiency, i.e. the proportion of current consumed by the side reaction instead of by the electrochromic reaction. If 100% of the positive current is used by the side oxidation reaction at the working electrode, no colour change will occur on this electrode and the transmittance will then account for the counter electrode change. In this case, the transmittance of the device will increase with the colouration

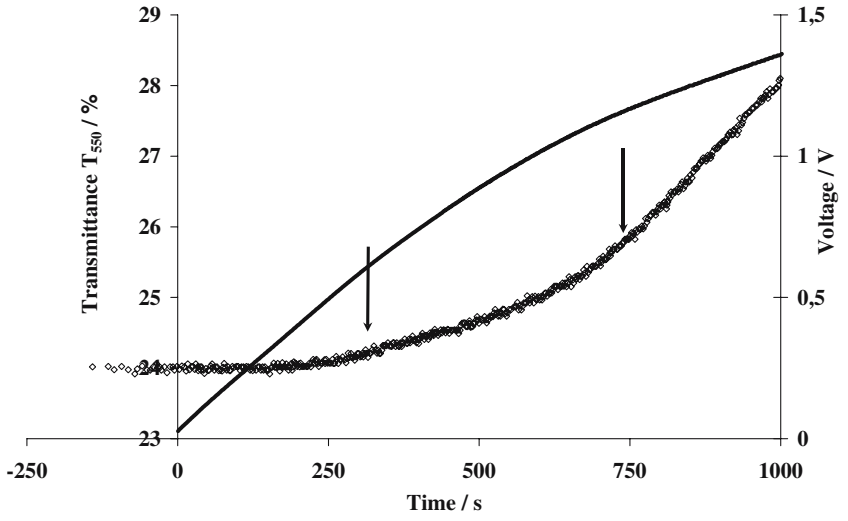

Fig. 5. Variation of the transmittance (◇) and voltage (continuous line) with time during a galvanostatic experiment at $+20\mu A\ cm^{-2}$ up to $+20\ mC\ cm^{-2}$ for a 40/120 IrO_2 symmetric device. The first arrow points out the moment when the change in transmittance exceeds 0.2%. The second arrow points out the beginning of a stabilized regime with linear variation of the transmittance.

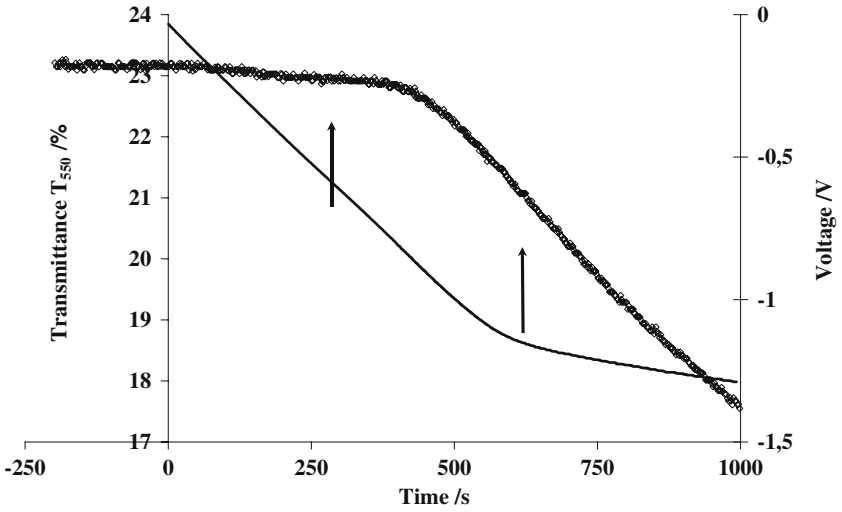

Fig. 6. Variation of the transmittance (◇) and voltage (continuous line) with time during a galvanostatic experiment at $-20\ \mu A\ cm^{-2}$ down to $-20\ mC\ cm^{-2}$ for a 40/120 IrO_2 symmetric device. The first arrow points out the moment when the change in transmittance exceeds 0.2%. The second arrow points out the beginning of a stabilized regime with linear variation of the transmittance.

efficiency of an IrO_2 layer (estimated at $15\ cm^2\ C^{-1}$). Thus the value of the experimental efficiency ($+7\ cm^2\ C^{-1}$) indicates that the side oxidation reaction consumes 45% of the total constant current. In the same way, the experimental efficiency in Figure 6 ($-10\ cm^2\ C^{-1}$) shows that the side reduction reaction consumes 65% of the total constant current.

3.8. *Potentials limits*

Charge limits of the safe operating window (no side reaction) are available from the transmittance versus time curves. They are deduced from the instant when deviation of transmittance happens (determined for a $\Delta T_{550} < 0.2\%$, see first arrow around 300 s on Figures 5 and 6). Starting from the short-circuited state, $+6.1\ mC\ cm^{-2}$ or $-5.5\ mC\ cm^{-2}$ can be safely exchanged. The maximum exchanged charge under safe conditions is then 11.6 mC cm^{-2}.

In order to convert these charge limits into potential limits, two steps are required:

- the insertion isotherm curve, the relationship between inserted charge and potential, will allow the conversion of exchanged charges into voltage changes and will therefore give a safe voltage window for the device. Due to its pseudo-capacitive behaviour the IrO_2 material exhibits a linear insertion isotherm. The following capacitance values will then be used to convert the exchanged charges into voltage changes:

$$\text{whole device}(1/C_{\text{device}} = 1/C_{\text{WE}} + 1/C_{\text{CE}})$$

$$C_{\text{device}} = 9.8\,\text{mF cm}^{-2}$$

$$\text{working electrode, 40 nm } IrO_2\text{ layer} \quad C_{40} = 13\,\text{mF cm}^{-2}$$

$$\text{counter electrode, 120 nm } IrO_2\text{ layer} \quad C_{120} = 40\,\text{mF cm}^{-2}$$

- the individual value of the potential of each layer versus a reference electrode in one state is then

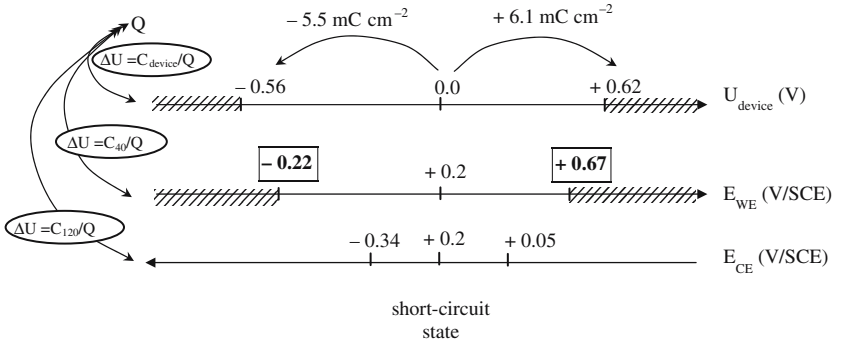

Scheme 1. Illustration of data treatment for the potential limits determination. The three horizontal arrows represent respectively the voltage of the 40/120 IrO_2 symmetric device, the potential versus SCE reference electrode of the working electrode (40 nm IrO_2 layer) and the potential of the counter electrode (120 nm IrO_2 layer). The middle of each horizontal arrow corresponds to the short-circuited state: the potential of each electrode is +0.2 V/SCE. The shaded parts correspond to voltage or potential ranges where side-reactions occur. The two safely exchanged charge densities (+6.1 and $-5.5\ mC\ cm^{-2}$) are reported on the top of the scheme. They are converted to voltages using the pseudo-capacitances reported in the text, C_{device},C_{40} and C_{120}, and reported respectively on each arrow started from the short-circuit state. or example for the worknScheme electrode, the $-5.5\ mC\ cm^{-2}$ corresponds to a voltage of −0.42 V (= −5.5/13); leading to the potential limit of −0.22 V/SCE (=0.2–0.42). The potential limits are the minimum of the two cathodic potential values (−0.22 and +0.05 V/SCE) and the maximum of the two anodic potential values (+0.34 and +0.67 V/SCE). In this case the two values are on the working electrode side.

required in order to give the corresponding safe potential window for each electrode. In order to determine the potential of both layers in one state, one symmetric materials device was exposed to short-circuit conditions immediately after manufacturing. The device was then dismantled and the polymer electrolyte removed from the two active layers. The potential of each layer was then measured in acidic solution. The same potential value was found for the two layers: +0.2 V/SCE. This is different from the +0.1 V/SCE potential in the precharging step in aqueous electrolyte.

Scheme 1 illustrates how to extract the safe potential window of an IrO_2 layer in contact with a polymer electrolyte (in V/SCE) using the previous discussion.

For one cycle at room temperature and dynamic conditions of $\pm$ 20 μA cm^{-2}, these limits are:

$$-0.2 < V < +0.7 \quad \text{V/SCE.} \tag{4}$$

This potential window is narrower than that determined by steady-state experiments in the acidic aqueous electrolyte [8, 9, 11]:

$$-0.25 < V < +1.1 \quad \text{V/SCE.} \tag{5}$$

These results are surprising. However other observations on real electrochromic devices confirm this behaviour and will be discussed below in terms of the nature of the side reactions.

3.9. *Reversibility of the side reactions in IrO_2 and WO_3 symmetric devices*

The last feature of the side reactions investigated in this work is the irreversibility. The irreversibility can be characterized through the remaining transmittance difference at the end of cyclic galvanostatic experiments.

Figure 7 shows the transmittance variation versus charge density during two cyclic galvanostatic experiments for a 40/120 IrO_2 device. In one experiment the charge density was cycled between 0 and +20 mC cm^{-2} by applying a constant current density of +20 μA cm^{-2} for the forward sweep and −20 μA cm^{-2} for the reverse sweep. In the second experiment, the charge density was cycled between 0 and −20 mC cm^{-2} by applying a constant current density of −20 μA cm^{-2} for the forward sweep and +20 μA cm^{-2} for the reverse sweep.

The extracted reversibility parameter is given in Table 2. As for the potential limits, it should be noted that this reversibility is very different at the oxide/polymer interface compared to that at the oxide/liquid electrolyte. In water, the oxidation is irreversible.

The analysis made on IrO_2 symmetric devices was not performed for WO_3 devices because the non pseudo-capacitive behaviour of this material prevents straightforward data treatment. We will only present the results of the side reaction irreversibility experiment, since it is remarkably different from that observed with IrO_2. Figure 8 shows the colouration response of a 200/800 WO_3 symmetric device with non-symmetric thicknesses in a galvanostatic experiment performed starting from the short-circuit state when +20 μA cm^{-2} up to +15 mC cm^{-2} then +20 μA cm^{-2} was applied. In contrast with IrO_2, since WO_3 is a cathodic colouring material, the darkening of the whole device during the first half of the experiment, corresponding to positive current, reveals a side oxidation reaction at the working electrode. With the WO_3 symmetric device, the reversibility of the side oxidation reaction is very poor (10% of reversibility with $\Delta TL_{max} = -5.5\%$ and $\Delta TL_{end} = -5.0\%$).

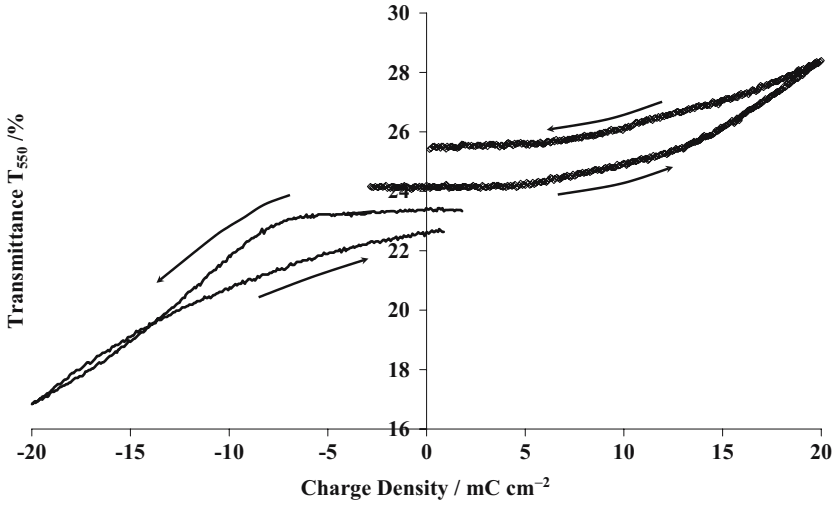

Fig. 7. Variation of the transmittance with charge density during a galvanostatic experiment for a 40/120 IrO_2 symmetric device. In the first experiment (◇) a constant current density of +20 μA cm^{-2} was applied until + 20 mC cm^{-2} had passed then the sign of the current was reversed to bring the charge density back to zero. In the second experiment (continuous line) a constant current density of −20 μA cm^{-2} was applied until −20 mC cm^{-2} had passed then the sign of the current was reversed to bring the charge density back to zero. Arrows show the direction of time increase.

Table 2. Global transmittance variations after + or −20 mC cm^{-2} on a 10/120 IrO_2 device and estimation of the reversibility of the side-reaction

Experiment	ΔTL_{max}/% after ± 20 mC cm^{-2}	ΔTL_{end}/% at 100% charge yield	Reversibility / %	Side reaction
+20 mC cm^{-2} then −20 mC cm^{-2} (Figure 7, ◇)	+4.2	+1.2	70	Oxidation
−20 mC cm^{-2} then +20 mC cm^{-2} (Figure 7)	−6.5	−0.7	90	Reduction

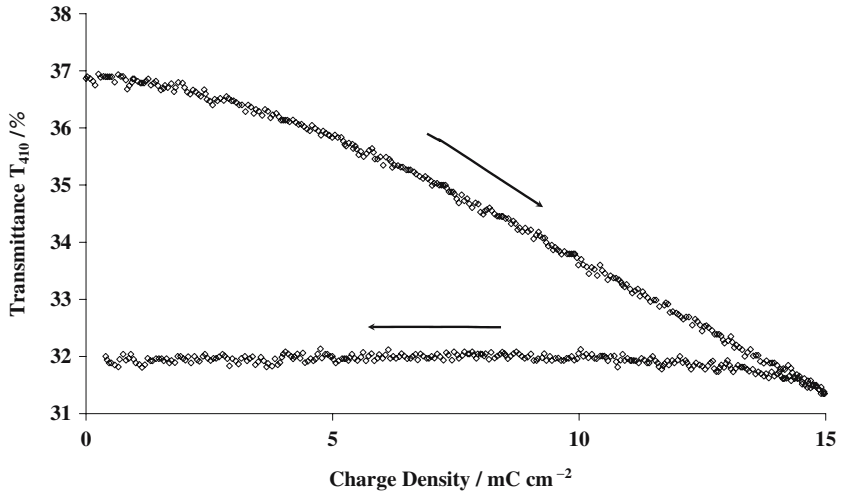

Fig. 8. Variation of the transmittance with charge density during a galvanostatic experiment for a 200/800 WO_3 symmetric device. A constant current density of +20 μA cm^{-2} was applied until + 15 mC cm^{-2} had passed then the sign of the current was reversed to bring the charge density back to zero. Arrows show the direction of time variation.

3.10. *Nature of side reactions*

As in aqueous electrolyte, the most probable anodic side reaction is the oxidation of water on both materials. However the observed difference in reversibility is indicative of different mechanisms.

In WO_3 symmetric devices, the behaviour is very similar to that observed in aqueous electrolyte, especially the very poor reversibility. The oxygen gas formed on WO_3 is probably quickly dissolved in the polymer electrolyte and diffuses away from the WO_3/polymer interface towards the bulk electrolyte. When the current is reversed the reduction of oxygen previously formed is rapidly limited by diffusion towards the electrode.

The good reversibility of the side reaction on IrO_2 and the abnormally low value of the potential where the side reaction occurs can be linked to other observations on real electrochromic devices with polymer electrolyte. When an as-deposited IrO_2 layer (almost completely oxidized) is put in contact with an acidic polymer electrolyte, spontaneous bleaching of the layer is observed. The as-deposited layer, which exhibits a potential of about +1.0 V/SCE, is then spontaneously reduced by a species which is oxidized at a potential lower than +1.0 V/SCE. This spontaneous bleaching of the as-deposited IrO_2 layer during manufacturing allows satisfactory functioning of a real WO_3/IrO_2 device made with as-deposited layers without a precharging step before assembly [4]. This behaviour may be associated with oxidation of water which does not produce oxygen gas but leads to an adsorbed form of oxygen "O" at the IrO_2/polymer interface:

$$H_2O \rightleftarrows \text{“O”} + 2e^- + 2H^+ \quad (6)$$

The low value of the reaction potential (+0.7 V/SCE) indicates that the formation of adsorbed oxygen would be easier than the formation of the oxygen molecule (thermodynamical potential around +1.0 V/SCE). This has already been observed for various other electrosorption reactions and especially for the oxidized platinum surface in acidic solutions in the anodic region before oxygen gas evolution [17]. If the potential is kept below the thermodynamic potential for oxygen evolution, water oxidation leads to a species which mostly stays at the interface (adsorbed form). When the current is reversed, this species will be easily reduced (no mass transport is needed) and this explains the good reversibility observed in this case.

3.11. *Comments on the design of electrochromic device*

The use of the potential limits and the limiting electrode in order to design electrochromic devices was first described by Rauh and coworkers [8, 9] and will not be detailed here. For an actual electrochromic window using WO_3 and IrO_2 materials, a contrast of 5 (for

example when the transmittance varies from 50% to 10%) is obtained when about 15 mC cm^{-2} is exchanged. The present results clearly show that a 40 nm IrO_2 layer is not sufficient to cycle the window without side reactions. The thickness of the IrO_2 layer in this type of device is often under-estimated. However the good reversibility of the side reaction on IrO_2 will partially hide the occurrence of these side reactions.

Other consequences for the design of electrochromic devices, especially on the bleached state transmittance, have also often been emphasized in previous work [18, 19]. In an actual WO_3/IrO_2 electrochromic device, the quasi-irreversible side reaction in oxidation on WO_3 may be used in order to adjust the charge balance between the electrodes and improve, for example, the transmittance under short-circuited conditions. This effect would be similar to the increase in transmittance in the bleached state observed at the beginning of an UV-exposure test on WO_3 electrochromic devices [20, 21]. The same irreversible oxidation on WO_3 occurs with light or an electrical driving force. However, even if this procedure (post-manufacturing transmittance adjustment) is easy and very efficient for the first cycles, its impact on the long term durability may be questionable.

4. Conclusion

This work shows that modifications of the optical properties of symmetric material devices constitute reliable tools to study *in situ* side reactions occurring at the electrochromic material/electrolyte interface. The transmittance changes are often more sensitive than the electrochemical changes or bubble appearance.

The study with *in situ* conditions (same interfaces as in an actual electrochromic window with a polymer electrolyte), shows that previously *ex-situ* determined values, in aqueous media, are not adequate: side reactions, which are irreversible in aqueous media, are partially reversible with a polymer electrolyte. This is particularly true for the overcharge of the IrO_2 electrode where reversibility can be as great as 95%.

The study of symmetric material devices would also be relevant to electrochromic devices in various other situations such as experiments performed under really dynamic conditions, experiments in solid state devices at different temperatures and experiments with a large number of cycles.

Finally, it is a general method for all types of electrochromic materials (oxides or polymers) and of electrolytes (oxides, polymers or liquids). The analysis performed on IrO_2 material is extendable to any electrochromic material. However, more complex data treatment would be required in order to take into account a hypothetical non constant colouration efficiency and a more complex insertion isotherm than the pseudo-capacitive one of IrO_2.

References

1. C.M. Lampert and C.G. Granqvist, Large Area Chromogenics: Materials and Devices for Transmittance Control' (Editors, SPIE Coloration Engineering Press, Bellingham, WA, 1990).
2. B. Buffat and F. Lerbet, *La recherche* **22** (1991) 434.
3. R.J. Mortimer, *Chem. Soc. Rev.* **26** (1997) 147.
4. R.D. Rauh, *Electrochim. Acta* **44** (1999) 3165.
5. C.M. Lampert, *Glass Sci. Technol.* **75** (2002) 244.
6. S. Taunier, C. Guery and J-M. Tarascon, *Electrochim. Acta* **44** (1999) 3219.
7. L-C. Chen and K-C. Ho, *Electrochim. Acta* **46** (2001) 2159.
8. R.D. Rauh and S.F. Cogan, *J. Electrochem. Soc.* **140** (1993) 378.
9. R.D. Rauh, *Solar Energy Mater. Solar Cells* **39** (1995) 145.
10. C. Lefrou, C. Gentilhomme, Proc. 190th meeting of the Electrochemical Society, San Antonio, USA, 6–11 October, 800, 1996.
11. R.D. Rauh and S.F. Cogan, in [1].
12. M.A. Petit and V. Plichon, *J. Electroanal. Chem.* **444** (1998) 247.
13. B.E. Conway, *J. Electrochem. Soc.* **138** (1991) 1539.
14. L.M. Schiavone, W.C. Dautremont-Smith, G. Beni and J.L. Shay, *J. Electrochem. Soc.* **128** (1981) 1339.
15. A. Azens and C.G. Granqvist, *J. Solid State Electrochem.* **7** (2003) 64.
16. C.G. Granqvist, E. Avendano and A. Azens, *Thin Solid Films* **442** (2003) 201.
17. J. O'M Bockris and S.U.M. Khan, *Surface Electrochemistry, A Molecular Level Approach* (Plenum Press, New York, 1993).
18. K.C. Ho, *Solar Energy Mater. Solar Cells* **56** (1999) 271.
19. K.S. Ahn, Y.C. Nah, J.Y. Park, Y.E. Sung, K.Y. Cho and S.S. Shin, *Appl. Phys. Lett.* **82** (2003) 3379.
20. C. Lefrou, O. Marrot and F. Garot, Proc. Materials Research Society Symposium, Boston, USA, 27 November-1st December (1995), Solid State Ionics IV, 369, 657.
21. C. Lefrou, F. Defendini, O. Marrot and F. Garot, Electrochromic window, FR 93-07096/EP94 401278/Pat No. 628849.